RSC Advances

Three novel biosorbents by modifying peanut shell for direct red 80 removal: Parameter optimization, process kinetics and equilibrium

Journal:	*RSC Advances*
Manuscript ID:	RA-ART-07-2015-014953
Article Type:	Paper
Date Submitted by the Author:	28-Jul-2015
Complete List of Authors:	zhang, lei; southwest petroleum university, chemistry and chemical engineering Cheng, Zhengjun; southwest petroleum university, chemistry and chemical engineering Guo, Xiao; southwest petroleum university, State Key Laboratory of Oil and Gas Reservoir Geology and Exploitation Jiang, Xiaohui; China West Normal University, Chemical Synthesis and Pollution Control Key Laboratory of Sichuan Province Li, Tian; China West Normal University, Chemical Synthesis and Pollution Control Key Laboratory of Sichuan Province

Graphical Abstract

In the study, three novel biosorbents (TEPA-PS, TETA-PS and DETA-PS) have been synthesized by epichlorohydrin and tetraethylenepentamine (TEPA), triethylenetetramine (TETA), or diethylenetriamine (DETA), and their preparation conditions were optimized by single factor test. Moreover, the process variables (such as initial concentration of the dye, temperature, and time of reaction) of DR80 removal onto the three biosorbents were optimized by RSM method, respectively. The experimental data of the three systems could be well-fitted to second order polynomial models and the three models were also examined using the analysis of variance and *t* test statistics, respectively. The results suggested that the three selected quadratic models in predicting the adsorption capacity of the dye were appropriate.

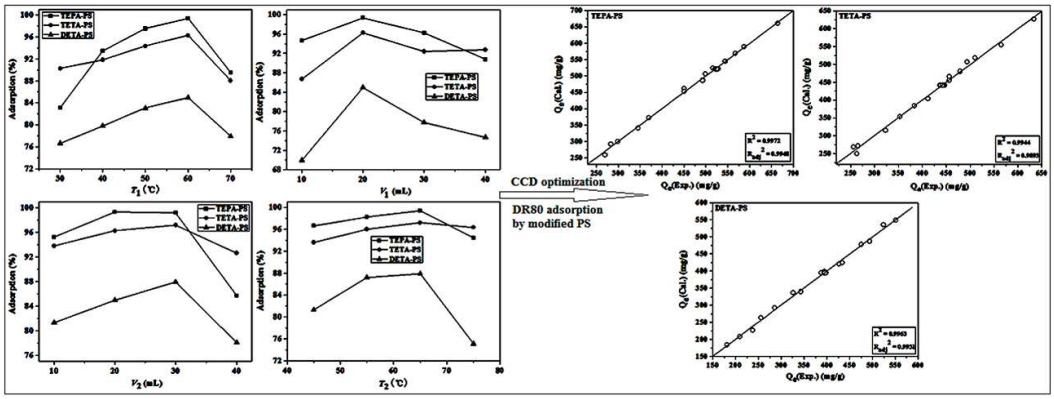

Three novel biosorbents by modifying peanut shell for direct red 80 removal: Parameter optimization, process kinetics and equilibrium

Lei Zhang [a, b, *], Zhengjun Cheng [a, b, c *], Xiao Guo [a], Xiaohui Jiang [c], Tian Li [c]

[a] *State Key Laboratory of Oil and Gas Reservoir Geology and Exploitation, Southwest Petroleum University, Chengdu 610500, Sichuan, China*

[b] *School of Chemistry and Chemical Engineering, Southwest Petroleum University, Chengdu 610500, Sichuan, China*

[c] *Chemical Synthesis and Pollution Control Key Laboratory of Sichuan Province, China West Normal University, Nanchong 637002, China*

*Corresponding author: ncczj1112@126.com(Z.J.C); zgc166929@sohu.com(L.Z.)

Abstract: In this study, we report three novel low-cost biosorbents based on modified peanut shells (TEPA-PS, TETA-PS and DETA-PS) prepared by epichlorohydrin and tetraethylenepentamine (TEPA), triethylenetetramine (TETA), or diethylenetriamine (DETA) as etherifying agent and crosslinking agent, respectively. A single factor test was employed to optimize the corresponding preparation conditions and hence obtain higher removal efficiency for direct red 80 (DR80) treatment. Consequently, a central composite design (CCD) was utilized to further analyze the individual and interactive effects of different process variables (such as initial concentration of the dye, temperature, adsorption time) in the adsorption capacity for dye removal onto above biosorbents. The corresponding experimental data could be simulated excellently using second order polynomial regression models due to high correlation coefficient values (R^2) of 0.9973, 0.9944 and 0.9960, low p-value of 0.000, and their F values of 404, 196 and 274 for the TEPA-PS, TETA-PS and DETA-PS biosorbents, respectively. As a result, the optimum conditions were found to be C_{DR80} = 145 or 143mg/L, T = 75°C and t = 161min for DR80 adsorption by TEPA-PS and TETA-PS, or DETA-PS. The measured maximum experimental adsorption capacities for DR80 under above optimum conditions were 690.18, 657.55 and 588.56 mg/g, which were in good agreement with their corresponding predicted values (679.96, 674.51 and 579.08 mg/g) owing to small relative errors of 1.48, -2.58 and 1.61%, respectively. In addition, many aspects of the kinetics and equilibrium isotherm of the dye adsorption onto modified PS were also investigated. The results indicate that pseudo-second-order and Langmuir models present the best fit to their kinetic and isotherm data. Finally careful thermodynamic investigations demonstrate adsorption processes based on modified PS are spontaneous and endothermic.

Keywords: Central composite design; Modified peanut shells; Direct red 80; Kinetics; Isotherm

Introduction

The last decades has seen an increasing interest of dye pollution with devastating effects on the

environment. In fact, currently more than seven million tons of dyes are annually produced in the world and extensively used in different industries (such as textile, paper, plastics, leather, food, pharmaceutical, cosmetics, dyestuffs, carpet, inkjet printing, *etc*.).[1] Such a large amount of dyeing effluents is released into river and hence causes long-term damaging effects on the environment upon which our society relies. In these dyes, azo dyes are the largest class of dyes, accounting for 60-70% of the total dyes consumption in business applications. However, a suitable disposal of azo dyes in the wastewater is quite difficult because they have one or more azo groups with aromatic ring and sulfonate groups which will induce high stability and resistance at oxidizing agent and aerobic digestion conditions, respectively. Reviews on current techniques for the dyes removal from wastewater including adsorption, coagulation, irradiation, ion exchange, electrolysis, biological treatment, advanced oxidation processes, electrochemical treatment, and so forth can be found in the literature.[2] Among them, the adsorption technique is a widely appreciated method, having advantages of simplicity, efficacy, effectively avoiding secondary pollution, and so on.[3] Although activated carbon adsorbent has promising performance for the dyes removal, there is certain limitation in practical application due to its high manufacturing cost and hard regeneration.[1] Therefore, to enhance removal efficiency of the dyes, development of low-cost efficient and practical adsorbents is absolutely desirable.

In recent years, some research groups have employed various adsorbents (such as modified walnut shell,[1] functionalized mesoporous silica material,[2] N-doped magnetic porous carbon,[3] PDDA/GO hydrogels,[4] $LaCO_3OH$,[5] low-cost alternative adsorbents,[6] Hydroxyl-functionalized ionic liquid-based cross-linked polymer (PDVB-IL-OH),[7] *etc*.) to remove dyes from aqueous solution. However, in these adsorbents, the agricultural and industrial wastes as adsorbents are attracted great attentions for the removal of dyes owing to their abundance and low prices.[8-12] Peanut shell (PS), an abundant agricultural residue, is produced annually for 4.5 million tons in China,[13] and has a complex material consisted of mineral, lipid, cellulose and polyphenol,[14] so it has been successfully utilized to remove heavy metals and dyes in the wastewater such as Zn (II) and Cd (II),[15] Se (□),[16] Cu (II),[15, 17, 18] Cr (□),[18] Pb (II),[15,19] Ni (II),[20] three cationic dyes (methylene blue, brilliant cresyl blue and neutral red),[21, 22] Reactive Black 5,[14] and three anionic dyes (amaranth, sunset yellow and fast green FCF).[23] Recently, a few researchers have modified PS based on different methods to improve their adsorption performance for the contaminants removal. For example, Liu et al.[13] has prepared a new absorbent (i.e. peanut shells were modified by epichlorohydrin and ethylenediamine) for Hg^{2+} and Cd^{2+} removals. The results indicated that the maximum removal efficiency of mercury by PS was merely 37%, while the removal efficiency of mercury based on MPS could reach 100% at 30min. Later, modified PS was synthesized by the

chemical reaction of epichlorohydrin and triethylenetetramine with raw PS as material, and it was used for Cr (VI) removal with high adsorption capacity (138.34 mg/g) in the column adsorption test.[24] The study of Ding et al.[25] implied that modified cotton (Cotton-alk, 69.5mg/g) exhibited the highest adsorption capacity for Pb(II) treatment, while modified peanut hull (Peanut-alk, 49.6mg/g) and cotton (Cotton-alk, 47.9mg/g) showed higher adsorption capacity for methylene blue (MB) removal than other biosorbents do. However, studies on modified PS for contaminants removal are still deficient, especially for the removal of anionic dyes.

In this paper, we propose an approach to prepare three novel biosorbents by modifying PS (TEPA-PS, TETA-PS and DETA-PS). The corresponding behaviors are characterized by FT-IR spectra and scanning electron microscopy (SEM) methods, and their preparation conditions were investigated. RSM combined with central composite design (CCD) was employed to design and optimize the process variables of DR80 adsorption onto the three biosorbents. In addition, the adsorption isotherms, kinetics and thermodynamic parameters for the dye removal by modifying PS were also discussed.

Materials and methods

Reagents

Tetraethylenepentamine (TEPA), Triethylenetetramine (TETA), Diethylenetriamine (DETA), and epichlorohydrin were purchased from Aladdin Chemistry Co., Ltd. (Shanghai, China). Direct red 80 (DR80, AR grade, Scheme 1) acquired from Alfa Aesar Tianjin Co., Ltd. (Tianjin, China), was used without further purification. It was dissolved in the distilled water (resistivity 18.25Ω· cm) to form solutions of 200 mg·L^{-1}. And its pH was regulated by HCl of 0.1mol·L^{-1} or NaOH of 0.1mol ·L^{-1} solution. Other chemical reagents were of analytical reagent grade, and distilled water was used throughout the experiment.

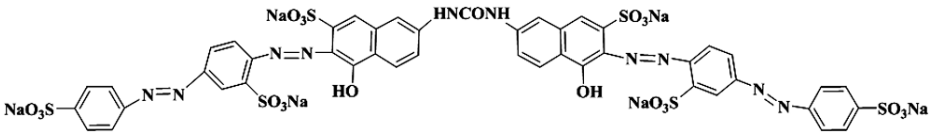

Scheme 1. Molecular structure of direct red 80

Synthesis of modified peanut shell

The peanut shells (PS) were obtained from Nanchong, China. Prior to modification, PS was extensively washed in running tap water for 2 h to remove coloration and dirt in its surface, and then boiled for 120 min to wipe off the residual seed capsule. Then they were washed with distilled water several times. The clean PS was transferred to a drying oven (Model: DHG-9070A, Shang Hai FeiYue Experiment Instrument Co., Ltd) set at 80°C for 24 h to reduce the water

content, then milled by a universal high-speed smashing machine and sieved using an 100-mesh sieve. The PS sieved was placed in a desiccator for further modification.

The modification of PS contains the following steps. Firstly, 20.0 mL of 1.25mol/L NaOH was blended with 10.0 mL epichlorohydrin on a shaker at 298.15K. Then, 1.20 g of clean PS powders was immersed in the solution for 1 h at 60°C equipped with thermostat. After the mixtures were washed several times by doubly distilled water to the eluent pH neutral, the obtained product (named as P1-PS) was dried at 70°C for 8h by a vacuum drying oven (Model: DZF-6020, Shang Hai YiHeng Scientific Instrument Co., Ltd). Secondly, the admixture solution with 20.0mL of 0.125 mol/L NaOH and 5.0mL of TEPA, 30.0mL of 0.125 mol/L NaOH and 5.0mL of TETA, or 30.0mL of 0.125 mol/L NaOH and 4.0mL of DETA was added into P1-PS powders obtained above. The mixtures were stirred at 65°C for 1.5 h followed by filtration and washing with doubly distilled water to remove excess TEPA, TETA, or DETA until the eluent pH reached almost neutral. Finally, the washed powders were dried at 70°C for 5 h by the vacuum drying oven, and they were named as TEPA-PS, TETA-PS and DETA-PS, respectively. The entire procedure was repeated three times to ensure the incorporation of TEPA-PS, TETA-PS, or DETA-PS. The three biosorbents were used for further characterization as well as DR80 adsorption studies. The modification process of PS involved chemical reactions was showed in Fig. 1.

Characterization of modified PS

FT-IR spectra of raw PS and modified PS surface before and after the adsorption of direct red 80 were carried out by a Nicolet-6700 FT-IR spectrometer (Nicolet, USA) based on potassium bromide sheets. And their corresponding surface property was also analyzed using SEM (JEOL-JSM-6510LV, Japan) and BET (Quantachrome ASIQ-C, USA) methods. Zero point charge (pH_{zpc}) of modified PS (TEPA-PS, TETA-PS and DETA-PS) was determined by the solid addition method.[26]

Adsorption experiments

The batch adsorption tests have been carried out in the laboratory by contacting a certain volume of DR80 solution (pH = 1.0-10.0) with different biosorbents (such as raw PS, TEPA-PS, TETA-PS and DETA-PS) at 180 rpm in a shaker and 343.15K for 180min to ensure apparent equilibrium. Three biosorbent doses change from 0.05 to 0.30 g/L were done to investigate the influences of its doses used for the DR80 removal, respectively. The suspensions were filtered when the equilibrium was obtained, and the complete UV-vis spectra scan of supernatant solutions was recorded using a UV-3600 spectrophotometer (Shimadzu, Japan) to avoid the error of fixed point determination. And the adsorption efficiency (%) and adsorption capacity are calculated by the

following equations:

$$\text{Adsorption}(\%) = (\frac{C_0 - C_e}{C_0}) \times 100 \quad (1)$$

$$Q_t = \frac{(C_0 - C_t)V}{W} \quad (2)$$

where C_0, C_e and C_t (mg/L) are the concentrations of dye at initial, equilibrium and time t, respectively; V (L) is the volume of solution; W (g) is the mass of adsorbent used; and Q_t (mg/g) is the amount of dye adsorbed onto adsorbent at time t.

Central composite design (CCD)

A second 3 factorial central composite design was employed to optimize the operational variables (such as initial concentration of dye, temperature and reaction time) of DR80 adsorption onto modified PS and analyze the effects of their interaction. It was amplified by six axial points (estimating the experimental errors and a measure of lack of fit), and six replications of center points (estimating the model curvature). And the preliminary range of process variables was ascertained by single factor test, respectively. Their range and levels were listed in Table 1. The adsorption capacity of dye (y) is selected as a response for the combination of independent variables, which is fitted by a second order polynomial model:

$$y = b_0 + \sum_{i=1}^{3} b_i x_i + \sum_{i=1}^{3} b_{ii} x_i^2 + \sum_{i=1}^{2} \sum_{j=1}^{3} b_{ij} x_i x_j \quad (3)$$

where b_0, b_i, b_{ii} and b_{ij} are regression coefficients (b_0 is constant term, b_i is linear effect term, b_{ii} is quadratic effect term, and b_{ij} is interaction effect term); x_i and x_j are the coded values of independent variables; and y is the predicted response value. Analysis of variance (ANOVA) was utilized to identify the accuracy and reliability of developed model, the significance of independent variables and their interactions. In addition, the chi-square (χ^2) test was performed to confirm whether there was a significant difference between the experimental and predicted values within the models. And it can be calculated from Eq. (4):

$$\text{Chi}^2 = \sum \frac{(Q_{\text{exp.}} - Q_{\text{pred.}})^2}{Q_{\text{pred.}}} \quad (4)$$

where $Q_{\text{exp.}}$(mg/g) and $Q_{\text{pred.}}$(mg/g) are the adsorption capacities of DR80 onto modified PS by experiment determined and model predicted, respectively.

Model validation and optimization

Validation set was employed to ascertain the predictive ability of the developed model. Moreover, the optimization of process variables was obtained for the DR80 system by the D-optimality index

in the Minitab 15.0 software.

Adsorption kinetics

The adsorption kinetics was carried on preliminary selected adsorbent, which was conducted by adding 20.0mg of TEPA-PS, TETA-PS, or DETA-PS into 100mL of the DR80 solution with different concentrations (100, 120 and 145 mg/L) and then shaking (180 rpm) for 3 h at 348.15K, and into 100mL of 145 mg/L DR80 solution and then shaking (180 rpm) for 3 h at different temperatures (318.15, 333.15 and 348.15K), respectively.

Four kinetic models were utilized to simulate the uptake of DR80 onto TEPA-PS, TETA-PS, or DETA-PS with time *t*, which are given as follows:

$$\ln(Q_e - Q_t) = \ln(Q_e) - k_1 t \quad (5)$$

$$\frac{t}{Q_t} = \frac{1}{Q_e} t + \frac{1}{k_2 Q_e^2} \quad (6)$$

$$\frac{t}{Q_e - Q_t} = \frac{1}{Q_e} t + k_3 t \quad (7)$$

$$Q_t = (1/\beta)\ln(\alpha\beta) + (1/\beta)\ln t \quad (8)$$

where Q_t (mg·g^{-1}) is the same as in Eq. (2); Q_e (mg·g^{-1}) is the equilibrium adsorption capacity; k_1 (min^{-1}), k_2 (g·mg^{-1}·min^{-1}) and k_3 (g·mg^{-1}·min^{-1}) are pseudo first order, pseudo second order and second order rate constants, respectively; α (mg·g^{-1}·min^{-1}) is initial adsorption rate; and parameter β (g·mg^{-1}) is related to the extent of surface coverage and activation energy.

Moreover, the intraparticle diffusion and liquid film models were applied to explore further the adsorption mechanism for DR80 removal onto the three biosorbents, and they are represented by Eq. (9) and Eq. (10), respectively.[27]

$$Q_t = k_{di} t^{0.5} + B \quad (9)$$

$$\ln(1 - F) = -k_{fd} t \quad (10)$$

where k_{di} (mg·g^{-1}·min$^{-0.5}$) is the rate constant of intraparticle diffusion; B is the intercept of Q_t *vs*. $t^{0.5}$ plot; k_{fd} (min^{-1}) is the rate constant of liquid film diffusion; and $F = Q_t/Q_e$.

Adsorption equilibriums

Batch equilibrium experiments have been performed for DR80 adsorption by TEPA-PS, TETA-PS, or DETA-PS at three temperatures. The same procedure was followed, but their initial concentrations altered from 101 to 145mg/L (with equal interval, 11.0 mg/L). Their amounts adsorbed at equilibrium (Q_e) are calculated by Eq. (11):

$$Q_e = \frac{(C_0 - C_e)V}{W} \quad (11)$$

Two-parameter isotherm models, i.e. Langmuir, Freundlich, Temkin and Dubinin-Radushkevich models are used for describing the adsorption behaviors of the dye onto TEPA-PS, TETA-PS, or DETA-PS. Their linear functions are expressed as:

Langmuir model: $$\frac{C_e}{Q_e} = \frac{C_e}{Q_m} + \frac{1}{K_L Q_m} \quad (12)$$

Freundlich model: $$\ln Q_e = \ln K_F + \frac{1}{n}\ln C_e \quad (13)$$

Temkin model: $$Q_e = \frac{RT}{b_T}\ln K_T + \frac{RT}{b_T}\ln C_e \quad (14)$$

The essential characteristics of Langmiur isotherm are expressed by a dimensionless equilibrium parameter, R_L ($R_L = 1/(1+ K_L C_0)$, C_0 is initial concentration of the dye, and K_L is the Langmuir constant). The type of isotherm is judged by R_L values, i.e. the adsorption equilibrium is irreversible ($R_L = 0$), favorable ($0 < R_L < 1$), linear ($R_L = 1$), or unfavorable ($R_L > 1$). [28]

Dubinin-Radushkevich model is utilized to further understand the adsorption mechanism of three adsorption reactions. Its linear model is given as follows:

$$\ln(Q_e) = \ln Q_m - \beta\varepsilon^2 \quad (15)$$

where ε ($\varepsilon = RT\ln(1+1/C_e)$) is the Polanyi potential; β ($mmol^2 \cdot J^{-2}$) is a constant related to the mean adsorption energy E ($E = \frac{1}{\sqrt{2\beta}}$).

In addition, three-parameter isotherm models (such as Sips and Redlich-Peterson isotherm) were also used. The Sips isotherm is a combination of Langmuir and Freundlich isotherm models, and it is expected to describe heterogeneous surfaces much better. At high concentration of adsorbate, it can predict a monolayer adsorption capacity characteristic of Langmuir isotherm. However, it reduces to the Freundlich isotherm at low amounts of concentration. It is presented: [29]

$$Q_e = \frac{K_S C_e^{\beta_S}}{1 + \alpha_S C_e^{\beta_S}} \quad (16)$$

where K_S(L/g) and α_S(L/mg) are the Sips model constants, respectively; β_S is the Sips model exponent.

Unlike Sips model, the Redlich-Peterson isotherm behaves like the Freundlich isotherm and come close the Henry's law at high and low concentrations of adsorbate, respectively. The model is listed as follows: [29]

$$Q_e = \frac{K_{RP} C_e}{1 + \alpha_{RP} C_e^{\beta_{RP}}} \quad (17)$$

where K_{RP}(L/g) and α_{RP}(L/mg) are the Redlich-Peterson model constants, respectively; β_{RP} is the Redlich-Peterson model exponent.

Results and discussion

Preparation of modified PS

To obtain better adsorption capacities of modified PS for DR80 removal, their preparation conditions (such as reagent dosage and temperature) have been optimized by single factor test. However, in the chemical reactions, the dosages of epichlorohydrin, TEPA, TETA and DETA are not only kept constant, but also their dosages are little excess. And time of reaction is long for the reactions. Therefore, the influences of reaction temperature and the amount of NaOH were investigated, respectively.

The effect of reaction temperature for modified PS preparation. Different reaction temperatures in the first cycle (Fig. 2) and the second cycle (Fig. 3) of the reactions were selected to synthesize various biosorbents, and their corresponding adsorption capacities were investigated for DR80 removal, respectively. As could be seen from Figs.2, 3, the three biosorbents prepared in the first step reaction temperature (60°C) and the second step reaction temperature (65°C) have the biggest removal efficiency (99.24 and 99.36, 96.27 and 97.20, and 84.95 and 87.92% for TEPA-PS, TETA-PS and DETA-PS, respectively) and adsorption ability (545.83 and 546.67, 529.46 and 534.60, and 467.20 and 483.57mg/g for TEPA-PS, TETA-PS and DETA-PS, respectively) for the DR80 system, possibly because the reactions (Figs. 2, 3) have higher yields with select temperature than those with other temperatures. Therefore, 60 and 65°C were selected as optimum reaction temperatures in the first and second step reactions of the three biosorbents preparation, respectively.

The effect of NaOH dosage for modified PS preparation. The amount of sodium hydroxide is an important factor to preparation of the three biosorbents, then its dosages have been studied and the results were shown in Figs.4, 5. In the first step reaction, the removal efficiency of DR80 onto modified PS rapidly increased and later gradually decreased with the increase in the amount of sodium hydroxide (from 10.0 to 40.0mL of 1.25mol/L NaOH), the phenomena possibly because the reaction between epichlorohydrin and celluloses from peanut hulls is more likely to happen during 20.0mL of 1.25mol/L NaOH than that during other dosages of sodium hydroxide (1.25mol/L). In the same way, for the second step reaction, their maximum adsorption capacities for DR80 removal were observed at 30.0 or 20.0mL of 0.125mol/L NaOH for TETA-PS and

DETA-PS, or TEPA-PS preparation. Therefore, the optimal amount of alkali is V_1 = 20.0mL (1.25mol/L NaOH), V_2 = 20.0mL (0. 125mol/L NaOH) for the TEPA-PS preparation, and V_1 = 20.0mL (1.25mol/L NaOH), V_2 = 30.0mL (0. 125mol/L NaOH) for the TETA-PS and DETA-PS preparations.

Characterization of modified PS prepared under optimum conditions

FT-IR spectra of raw PS, chemically modified PS, only dye (DR80), and the dye loaded modified PS were listed in Fig. 1S (Supporting information). As could be seen from Fig. 1S (A), the broad mixed stretching vibration adsorption band of amino and hydroxyl groups at 3396 cm^{-1} was reduced by the chemically modified treatment. It is observed that etherification could bring the reduction of stretching vibration adsorption band of carboxyl group (-OH) at 1700 cm^{-1}. The peak around 1270 cm^{-1} is assigned to the stretching vibration adsorption band of C-N, which corresponds to the amine groups in the framework of modified PS.

However, there are a few peaks in the spectra taken after the dye adsorption, and these peaks refer to modified PS-DR80 complex and DR80 molecule (Fig. 1S (B)), i.e. the peaks at 1476 cm^{-1} and 617 cm^{-1} are assigned to the characteristic peaks of aromatic ring; and the peak at 1126 cm^{-1} is due to the asymmetric vibration of sulfonate. However, their corresponding peak ratios and locations altered after DR80 was adsorbed onto modified PS (1482, 620 and 1116 cm^{-1} for TEPA-PS, 1481, 619 and 1117 cm^{-1} for TETA-PS, and 1486, 626 and 1110 cm^{-1} for DETA-PS). This fact indicated that the interactions between the adsorbed dye anions ($R\text{-}SO_3^-$) and protonated amino group ($R'\text{-}NH_3^+$) of modified PS or H^+ ions on their external surface were carried through the sulfonate groups.

Fig. 2S (a-g) (Supporting information) shows scanning electron micrographs (SEM) of raw PS, modified PS, and modified PS adsorbing the dye. It is clear from the SEM figures that modified PS has rougher external surface and more different size pores than raw PS has, which are in good agreement with their corresponding results of BET analysis (The surface area of raw PS and modified PS (TEPA-PS, TETA-PS and DETA-PS) is 1.381 and (6.095, 3.747 and 3.611) m^2/g, respectively), implying that the modification changes its surface structure and increases the adsorption capacity of modified PS for DR80. However, when modified PS adsorbed the dye, its surface become smoother (Fig. 2S (e-g)) due to electrostatic interactions between sulfonate groups of the adsorbed dye and $R'\text{-}NH_3^+$ of modified PS or H^+ ions on its external surface. After the adsorption reaction happens, its surfaces are covered with the dye molecules.

Biosorption capacity for the direct red 80 adsorption

In this study, a preliminary screening of four biosorbents (Table 2) was investigated to have a

comparative measure of the biosorption efficiency for the DR80 system. It could be seen from Table 2, modified PS (such as TEPA-PS, TETA-PS and DETA-PS) has bigger adsorption ability (from 569.06 to 651.86mg/g) and adsorption efficiency (in the range of 81.29-93.12%) for DR80 removal than those of raw PS. Because amine groups on the surface of modified PS were easily protonated ($R'\text{-}NH_3^+$) under acidic condition, the anionic dye could be removed more rapidly through electrostatic force. Moreover, the removal efficiency for DR80 onto the three biosorbents followed the order TEPA-PS > TETA-PS > DETA-PS probably because the surface area of TEPA-PS (6.095 m^2/g) are higher than those of TETA-PS (3.747 m^2/g) and DETA-PS (3.611 m^2/g), and their surface area decrease followed the order DETA-PS < TEPA-PS < TETA-PS (2.896, 0.807 and 2.108 m^2/g for DR80 adsorption onto DETA-PS, TEPA-PS and TETA-PS, respectively). Therefore, TEPA-PS, TETA-PS and DETA-PS are chosen for further experimental analysis regarding kinetics, isotherms, and the optimum operational variables for DR80 adsorption onto modified PS.

Influence of pH and modified PS dosage on adsorption efficiency for the direct red 80 system

In the adsorption process, solution pH can affect the degree of ionization, the surface charge of adsorbent, and speciation of adsorbate, so DR80 adsorption has been studied with different pH (from 1.0 to 10.0) (Fig. 3S, Supporting information). As could be seen in Fig. 3S, the removal efficiency of DR80 decreased with the increase in pH of solution. Moreover, the maximum removal efficiency of the dye was observed at pH 2.0 (92.43%, 89.69% and 80.78% for TEPA-PS, TETA-PS and DETA-PS, respectively). This could be attributed to zero point charge (pH_{zpc}) of modified PS (Fig. 4S, Supporting information).[30] The solution pH can affect groups distributed (such as amine, hydroxyl and carbonyl groups) on the surface of modified PS. At low pH, the amine groups ($R'\text{-}NH_2$) of modified PS could be protonated by H^+ ions in the solution. In addition, the DR80 was dissolved and its sulfonate groups were dissociated ($R\text{-}SO_3^-$). Then the adsorption process proceed by the electrostatic interaction between $R\text{-}SO_3^-$ and protonated amino group ($R'\text{-}NH_3^+$) of modified PS. Adsorption sites increase with decreasing the solution pH due to more amine groups protonation of modified PS, which would induce that the adsorption capacity of DR80 onto modified PS enhanced. The result was in good agreement with the reported anionic dye removal onto MWNS.[1] However, at high pH, the protonated amine groups' amount decreases and more OH^- ions are available to compete with the anionic sulfonic groups, so the removal of the dye will decrease at high pH. As suggested above, pH 2.0 was selected for later studies.

The influence of different biosorbent dosages on the DR80 removal efficiency was shown in Fig. 6. As evident from Fig. 6, the removal rate of the dye increased obviously (from 39.44 to 93.12%, 27.88 to 90.10%, and 25.32 to 81.29% for TEPA-PS, TETA-PS and DETA-PS,

respectively) with increasing biosorbent dosages (from 0.05 to 0.20 g/L), and their corresponding adsorption capacities decreased significantly (from 1104.24 to 651.86 mg/g, 780.74 to 630.68 mg/g, and 708.86 to 569.06 mg/g for TEPA-PS, TETA-PS and DETA-PS, respectively). However, as the modified PS dosages were further raised in the range of 0.20-0.30 g/L, no remarkable increment in the removal tendency was observed. This behavior could be explained due to the adsorbent particles agglomeration and the increase in diffusion path length with increasing its dosages.[30] Therefore, taking the removal efficiency of DR80 and economy into account simultaneously, 0.2 g/L of modified PS was selected for further studies.

Response surface experiments

Statistical analysis and regression model. Compared to traditional single parameter optimization, response surface methodology (RSM) is far more advantageous in saving time, space and raw material. Table 3 illustrated the experimental conditions and the adsorption capacity of DR80. The regression coefficients, sum of squares, *T*-value, and PC values of the three models were listed in Table 1S (Supporting information). By substituting the coefficients in Eq. (3) with their values from Table 1S, three best fitted models for the TEPA-PS (Eq. (18)), TETA-PS (Eq. (19)) and DETA-PS (Eq. (20)) systems were given as follows:

$$y(\text{mg/g}) = 521.828+28.737\times x_1+118.690\times x_2+33.075\times x_3-22.010\times x_1^2-51.338\times x_2^2 -12.685\times x_3^2+30.830\times x_1x_2+17.825\times x_1x_3-5.758\times x_2x_3 \quad (18)$$

$$y(\text{mg/g}) = 440.773+24.859\times x_1+114.541\times x_2+38.221\times x_3-4.168\times x_1^2-19.313\times x_2^2 -5.726\times x_3^2+21.083\times x_1x_2+14.415\times x_1x_3+1.362\times x_2x_3 \quad (19)$$

$$y(\text{mg/g}) = 394.553+24.309\times x_1+123.496\times x_2+35.121\times x_3-16.563\times x_1^2-9.049\times x_2^2 -8.975\times x_3^2+10.555\times x_1x_2+0.963\times x_1x_3-5.215\times x_2x_3 \quad (20)$$

where y expresses the adsorption capacity of DR80; x_1, x_2, and x_3 denote initial concentration of the dye, temperature, and time of adsorption reaction, respectively.

Analysis of variance (ANOVA) method was applied to further explore the significance and accuracy of the three models (Eqs. (18-20)) and the calculated results were shown in Table 2S (Supporting information). From Table 2S, the three models were statistically significant due to high F values (F_{model} = 404, 196 and 274) and a very low p-value (p_{model} = 0.000). The significant lack of fits ($p < 0.05$) indicated that there might be some systematic variation unaccounted for in the hypothesized models. This was thought to be owing to the exact replicate values of the independent variable in the model that provided an estimate of pure error.[31] Besides, to verify whether the three models obeyed a normal distribution or not, normal probability plots of the residuals (Fig. 5S, Supporting information) were also used. The regression data on Fig. 5S fitted almost near to a straight line, indicating that the hypothesis of analysis was fulfilled. Fig. 7

showed the plots of the experimental versus predicted values. It could be seen from Fig. 7, the predicted values by Eqs.(18-20) were in good agreement with their corresponding experimental values for DR80 adsorption onto modified PS. The correlation coefficient values (R^2) were 0.9973, 0.9944 and 0.9960, implying that only 0.27%, 0.56% and 0.40% of the total variations couldn't be elucidated from three regression models, respectively. Their corresponding adjusted correlation coefficient values (R^2_{adj} = 0.9948, 0.9893 and 0.9923) were close to 1.0, demonstrating that Eqs.(18-20) have high reliability for predicting their experimental data, respectively. Moreover, the predicted chi-square values ($\chi_{pred.}^2$ = 1.54, 2.75 and 2.30 for TEPA-PS, TETA-PS and DETA-PS, respectively) were lower than the tabulated chi-square value ($\chi_{tab\ (\alpha;\ df\text{-}1)}^2 = \chi_{tab\ (0.05;\ 19)}^2$ = 30.144), which indicated no significant difference between the experimental and predicted values. The chi-square (χ^2) test again corroborated with 95% confidence level that the three models proposed were adequate to fit their relevant experimental data.

To further estimate the predicted ability of three models (Eqs.(18-20)), the validation set with three independent variables (Table 4) was designed by Taguchi design matrix. From Table 4, the adsorption capacities of DR80 altered from 412.56 to 598.90mg/g, 358.68 to 538.10mg/g and 306.56 to 480.24mg/g for the TEPA-PS, TETA-PS and DETA-PS biosorbents, respectively. Fig. 8 represented the experimental *vs.* predicted value plots of the validation sets. The results predicted by the three models were in good agreement with their corresponding experiments owing to high correlation coefficients and low standard deviation (*SD*) (R^2 = 0.9931, *SD* = 6.2124 for the TEPA-PS biosorbent, R^2 = 0.9952, *SD* = 5.1071 for the TETA-PS biosorbent, and R^2 = 0.9918, *SD* = 6.9630 for the DETA-PS biosorbent), suggesting that the three selected quadratic models in predicting their corresponding adsorption capacities were satisfactory.

In addition, the significance of the three models coefficients (Table 2S) was also discussed based on their Student's *T* test and *p*-values. According to the obtained *p*-values (Table 2S), for the TEPA-PS and TETA-PS systems, their linear terms (x_1, x_2 and x_3) were observed to be statistically significant ($p < 0.05$), and only the interaction (x_2x_3) was no statistically significant at the 95% confidence level, which could be explained by their interaction effect plots (Fig. 6S (A) and (B), see support information) due to the parallel line of $x_2 x_3$. It could be seen in Fig. 6S (A) and (B); other interactive terms x_1x_2 and x_1x_3 are nonparallel lines, implying that there were the interactions between the two factors, respectively. However, for the DETA-PS system, Fig. 6S (C) and its *p*-values (Table 2S) indicated that there was the interaction between initial concentration of the dye and temperature (x_1x_2) and other interactive terms (such as x_1x_3 and x_2x_3) were no statistically significant. It is evident that all linear and quadratic terms were statistically significant ($p < 0.05$) for DR80 adsorption onto DETA-PS. Moreover, the main effects of all the three

independent variables were more significant than their corresponding quadratic effects for the three adsorption models because they have higher PC values. As could be seen from Table 1S, we detected that temperature (x_2) has the maximal contribution (71.92%, 82.03% and 86.84% for TEPA-PS, TETA-PS and DETA-PS, respectively) for DR80 removal, which could be explained by their main effect plots (Fig. 7S, Supporting information) because their factors (x_2) have a very steep slope. The *T*-value and *p*-value obtained (Tables 1S, 2S) showed that all the three variables have a direct relationship for DR80 adsorption by TEPA-PS, TETA-PS and DETA-PS, respectively.

Effects of process variables. To better study the effects of independent variables and interactions between all three variables, three dimensional response surfaces and two dimensional contours were given in Figs. 8-13S (a-c) (Supporting information), respectively. From Figs. 8S-10S (a, e), the effect of temperature was remarkable for DR80 removal on TEPA-PS, TETA-PS, or DETA-PS. The dye uptake increased markedly with elevating the temperature that could be related to the endothermic nature of three adsorption reactions. The results were well consistent with the ANOVA analyses for the three systems. Endothermic reaction for some dyes onto different adsorbents has been reported. For example, the adsorption of Reactive Black 5 (RB5) onto peanut hull, [14] methylene blue onto Au-NP-AC, [32] and reactive blue 2 onto eco-friendly semi-IPN biocomposite hydrogel (EBH) [33] were found to be endothermic.

The effect of the dye concentrations on the DR80 removal by modified PS was shown in Figs. 8S-10S (a, b). The adsorption capacities of the dye increased with increasing its initial concentration, and their maximum adsorption capacities were obtained at the maximum dye concentration (145mg/L) except for the DETA-PS adsorbent, which is mainly due to the increase in mass transfer from the concentration gradient and enhancing the interaction between adsorbent and the dye. Almost an ellipse or saddle nature lines in their contour plots (Figs. 11S-13S (a, b), Supporting information) implied that there were the interactions of the dye concentration with temperature and the dye concentration with the reaction time for DR80 removal onto TEPA-PS or TETA-PS. But the contour plot (Figs. 13S (b)) was almost circular arc lines which indicated no significant interaction between the concentration of dye and the reaction time for DR80 adsorption onto DETA-PS.

Figs. 8S-10S (b, c) listed the effect of adsorption reaction time for DR80 removal by modified PS. As could be seen from Figs. 8S-10S (b, c), the adsorption capacity of DR80 onto modified PS increased quickly in first 49 min (-1.25 point), and then rose slowly to reach the equilibrium. This might be explained by a rapid adsorption on the exterior surface of modified PS, and then the dye molecules would be transferred to internal sites of the adsorbent by pore diffusion, therefore it will

require a longer time. According to 3D surface and 2D contours plots, the maximum adsorption capacities (mg/g) were obtained at higher dye concentration, temperature and contact time. In addition, from Figs. 11S-13S (c), there was no significant interaction between temperature and the adsorption time for DR80 removal onto TEPA-PS, TETA-PS, or DETA-PS owing to almost a circular arc presenting their contour plots.

Process optimization of the DR80 removal. Minitab 15.0 software is employed to optimize the independent variable values that can obtain a maximum response. The optimality plots for response variable values were shown in Fig. 14S (Supporting information). The composite desirability values of the dye concentration, *T*, and adsorption time gradually increased and subsequently reached a peak value. Therefore, the adsorption capacity of DR80 by TEPA-PS, TETA-PS, or DETA-PS was attained the maximum response value at high initial concentration of DR80 level, high *T*, and long adsorption time. In summary, a *D*-optimality of 0.9824, 0.9965, or 1.0000 with the maximum response value of 679.96, 674.51, or 579.08mg/g was discovered at C_{DR80} = 145 or 143mg/g, T = 75°C, and t = 161min for DR80 adsorption onto TEPA-PS, TETA-PS, or DETA-PS. In addition, six additional experiments for the dye adsorption on modified PS were done to confirm the experimental data were not biased toward the predicted values under the aforementioned optimum conditions, respectively. Their average experimental values were 690.18, 657.55 and 588.56 mg/g for the TEPA-PS, TETA-PS and DETA-PS biosorbents, which were in good agreement with the predicted values by the three regression models, with small relative errors of 1.48%, -2.58% and 1.61%, respectively. The result suggested that the three models proposed (Eqs. (18-20)) were adequate for reflecting the expected optimization.

Adsorption kinetics for the direct red 80 system

Figs. 15S-16S (Supporting information) displayed the changes of adsorption capacity with time at different initial concentrations of the dye and temperatures for the TEPA-PS, TETA-PS, and DETA-PS systems, respectively. The adsorption capacities of DR80 increased quickly in the first 40min and then rose slowly until the equilibrium was reached at 150min for the six systems.

The adsorption kinetics data for the three systems at different conditions were discussed by four kinetics models (such as pseudo first order, pseudo second order, second order and Elovich models) and their relevant kinetic parameters were calculated and listed in Table 5. As evident from Table 5, the kinetics data of DR80 adsorption onto modified PS were represented better by pseudo second order model than those by other models because their correlation coefficient values were exceedingly high ($R^2 > 0.990$, Table 5), and their fitted values ($Q_{e,\,fit}$) based on Eq. (6) showed a good agreement with the corresponding experimental values ($Q_{e,\,exp}$). Similar results were reported for DR80 adsorption by almond shells and AC/DDAC.[34] In addition, the initial

adsorption rates of DR80 (h, $h = k_2 Q_e^2$) [35] are calculated by their pseudo second-order rate constants, respectively. The h values for the three systems decreased with augmenting initial concentration of the dye. The reason for this phenomenon might be attributed to lower competition for the surface active sites at lower concentration of the dye. By contrast, at higher dye concentration, the competition for the adsorption sites is high, and then lower adsorption rate would be attained. At the same time, the three adsorption reactions were endothermic because their h values increased with a rise of reaction temperature.

In addition, the experimental data for DR80 adsorption onto TEPA-PS, TETA-PS, or DETA-PS were also evaluated by Elovich model. The results suggested that the Elovich equation might be used for predicting the adsorption kinetics data of DR80 at high initial dye concentration and temperature by modified PS probably because the three biosorbents all possess heterogeneous surface active sites.

Moreover, intraparticle diffusion model was employed to investigate the diffusion mechanism of DR80 removal onto modified PS at different conditions. The plots of Q_t *vs.* $t^{0.5}$ (Fig. 9 and Fig. 17S) were nonlinear in the whole time range, but they could be separated into two linear regions, implying that the multistage adsorptions should happen for the three adsorption reactions at different conditions. The first linear portion of the plots (Fig. 9 and Fig. 17S) expressed external surface adsorption, i.e. the dye molecules were transported to the external surface of modified PS by the film diffusion. At this stage, the instantaneous adsorption with a high removal rate was probably owing to a strong electrostatic attraction between the external surface of modified PS and DR80 molecules. The second linear portion of the plots was a gradual adsorption stage where intraparticle diffusion was rate-limiting, and then when the adsorption reactions were slowly close to equilibrium, their intraparticle diffusion rates started to slow and become stagnant because all the active sites of modified PS were occupied by the dye molecules. These steps showed that both film diffusion and intraparticle diffusion might occur simultaneously. At the same time, the adsorption kinetics data of the three systems were the best fitted by pseudo second order model, reconfirming that two or more steps were involved in the three adsorption reactions. However, the linear plots at each concentration and temperature did not pass through the origin (Table 3S, Supporting information), which implied that the intraparticle diffusion was not the only sole rate-controlling step for DR80 adsorption onto modified PS, but also the film diffusion might control the dye adsorption rate due to the large intercepts of the first linear portion of the plots (Table 3S). Eskandarian et al. [36] reported similar results for DR23 and DB86 adsorptions onto CNT-Den. Additionally, the k_{di} values of DR80 rose with enhancing their initial concentrations (Table 3S), suggesting that the heightened driving force at high initial dye concentrations might

increase the intraparticle diffusion of the dye onto TEPA-PS, TETA-PS, or DETA-PS.

The liquid film model was utilized to explore which one showed a greater influence on the uptake rate of DR80 by modified PS. The plots of ln(1-*F*) versus *t* for DR80 adsorption by TEPA-PS, TETA-PS, or DETA-PS at different conditions were shown in Fig.10 and Fig. 18S (Supporting information). If the plots of Fig.10 and Fig. 18S are linear and pass through the origin, then the slowest step in the adsorption process is governed by a film diffusion; otherwise it is controlled based on the intraparticle diffusion. As could be observed from Fig.10 and Fig. 18S, although all of the film diffusion plots showed good linear relationships, none of the line segments passed through the origin (Table 3S), which suggested that the intraparticle diffusion controlled the adsorption rates of the three adsorption processes at different conditions.

Adsorption isotherms for the direct red 80 system

In the present study, the dye biosorption capacity as a function of dye concentration (101-145 mg/g) at equilibrium state with different temperatures has been analyzed by very common two-parameter models of Langmuir, Freundlich, Temkin and Dubinin-Radushkevich and three-parameter models of Radke-Prausnitz and Sips adsorption isotherms. All the model parameters were calculated by linear or non-linear regression based on MATLAB software (Table 6) and their plots were shown in Fig. 11 and Figs. 19S, 20S (Supporting information).

It is evident from Fig. 11 and Figs. 19S, 20S that the experimental data could be fitted better at different temperatures by Langmuir isotherm model than those by other models. The Freundlich constant (K_F) increased with rising the temperature, implying that the three adsorption processes were endothermic. Moreover, their corresponding *n* values were in the range of 1-10 (Table 6), which indicated that the dye adsorption onto TEPA-PS, TETA-PS, or DETA-PS was favorable. The b_T values (Table 6) from Temkin isotherm suggested that the chemical adsorptions were involved in the three adsorption reactions.[37] Langmuir constant (K_L) increased with rise in the temperature, representing stronger attractions between the active sites of modified PS and DR80, also indicating a higher affinity between modified PS and the dye molecules at higher temperature than that at lower temperature.[38] At different initial concentrations of the dye and temperatures, their R_L values altered from 0.0037 to 0.0708, which further confirms that Langmuir adsorption isotherm is applicable for the three adsorption processes. For the DR80 removal, its monolayer adsorption capacities augmented (from 561.80 to 719.42 $mg \cdot g^{-1}$, 500.00 to 694.44 $mg \cdot g^{-1}$, and 502.51 to 617.28 $mg \cdot g^{-1}$ for the TEPA-PS, TETA-PS, and DETA-PS biosorbents, respectively) with rising the temperature (from 318.15 to 348.15K), reconfirming that the three adsorption processes are endothermic reaction. This result indicates that the modified PS possesses high capabilities to remove DR80 from aqueous solution.

The equilibrium data were also evaluated using Dubinin-Radushkevich isotherm model. Although the fits were not as good as those of Langmuir isotherm, the mean adsorption energy (E) values can provide information about the adsorption mechanism of the three reactions. As listed in Table 6, the values of E were greater than 8 kJ·mol^{-1}for the three systems, suggesting that the three adsorption reactions were controlled by chemical adsorption mechanism.[39] In addition, three-parameter adsorption isotherm models also showed an excellent fit to the experimental equilibrium data of the three systems at high temperature due to high R values (Table 6).

To explore the adsorption efficiency of modified PS as biosorbents for the uptake of DR80 from aqueous solution, the Q_{max} (mg/g) values of modified PS were compared with various reported adsorbents (Table 4S, Supporting information). As could be seen from Table 4S, the adsorption capacities of TEPA-PS, TETA-PS and DETA-PS (719.42, 694.44 and 617.28 mg/g for DR80) are better than those of other reported adsorbents except for poly (amidoamine-co-acrylic acid) copolymer (PAC). This result indicates that the modified PS can be considered as promising biosorbents for DR80 removal from printing and dyeing sewage.

Thermodynamic studies

The van't Hoff analysis was applied to expose the spontaneity of DR80 adsorption onto the modified PS and obtain thermodynamic parameters (such as ΔH^o, ΔS^o and ΔG^o).

$$\ln K_c = -\frac{\Delta H^0}{RT} + \frac{\Delta S^0}{R} \quad (21)$$

$$\Delta G^0 = \Delta H^0 - T\Delta S^0 \quad (22)$$

where K_c (L/mol) is the thermodynamic adsorption equilibrium constant and equals to Q_e/C_e [28]. The of ΔH^o and ΔS^o values are calculated from the slope and intercept of $\ln K_c$ *vs.* $1/T$ plots, respectively (Figs. 21S, Supporting information).

The thermodynamic parameter values obtained for the three systems were reported in Table 7. Negative values of ΔG^o validated the feasibility and spontaneous nature of the three adsorption processes at all the studied temperatures. The increase in the absolute values of ΔG^o with rising the temperature implied that the adsorption of DR80 onto modified PS was more favorable at higher temperature than those at lower temperature. The positive values of ΔH^o and ΔS^o confirmed the endothermic nature of the dye adsorption process and an increase in the degrees of freedom at the solid-liquid interface during the dye adsorption on the active site of modified PS, respectively. It was noticed that the values of ΔH^o, K_L and Q_m for the TEPA-PS biosorbent were bigger than those for the TETA-PS and DETA-PS biosorbents (Tables 6, 7), which indicated that the affinity of DR80 with TEPA-PS was stronger than that of DR80 with TETA-PS or DETA-PS.[36]

Generally, the adsorption on solids is classified as either physical adsorption or chemical

adsorption, which are often identified by the change in free energy ($\Delta G°$) of the adsorption reaction, i.e. the adsorption reaction is dominated by the physical adsorption when its $\Delta G°$ values are in the range between -20 and 0 kJ·mol^{-1}; for the chemical adsorption, the $\Delta G°$ values alter from -80 to 400 kJ·mol^{-1}.[40] As could be seen from Table 7, their $\Delta G°$ values implied that the physical adsorption might control DR80 removal from wastewater by TEPA-PS, TETA-PS and DETA-PS, respectively. The ΔH^o values of the three systems confirmed the involvement of electrostatic interaction in the DR80 adsorption onto modified PS due to their ΔH^o values in the range of 20-80 kJ/mol.[40]

Measurement of sticking probability for the direct red 80 system

The apparent activation energy (E_a) and sticking probability (S^*) for DR80 adsorption onto the surface of modified PS are evaluated by Eq. (23):[41]

$$S^* = (1-\theta)\exp(-\frac{E_a}{RT}) \qquad (23)$$

where θ expresses the surface coverage and equals to 1-C_e/C_0. The sticking probability (S^*) is a function of the adsorbate/adsorbent system but it must lie in the range of 0-1. The values of E_a and S^* were evaluated from the slope and intercept of ln (1-θ) *vs*. 1/T plots (Figs. 22S, Supporting information), and their corresponding values were listed in Table 7. The positive E_a values implied that the three adsorption reactions are more likely to occur at higher solution temperature and they are endothermic in nature. The sticking probability of DR80 onto the modified PS is very high due to their values of S^*<<1.[41]

Isosteric heat of adsorption for the direct red 80 system

In the text, Clausius-Clapeyron equation (Eq. 24)[42] were employed to calculate the isosteric heats of DR80 adsorption onto the modified PS at constant surface coverage (Q_e = 405, 425, 445, 465, and 495mg/g).

$$Q_{st} = R\frac{d\ln C_e}{d(1/\mathrm{T})}\Big|_{Q_e} \qquad (24)$$

where Q_{st} (kJ/mol) denotes the isosteric heat of adsorption at a specific solute loading Q_e (mg/g); C_e (mg/L) is the equilibrium concentration of adsorbate in dilute solution, which is obtained at a given adsorbed amount in the solid phase (Q_e) by Langmuir isotherm model with the obtained parameters in Table 6.

The values of Q_{st} were determined from the slope of the lnC_e-1/T plot for different amounts of DR80 onto the modified PS (Figs. 23S, Supporting information), and their corresponding Q_{st} values were shown in Table 8. As evident from Table 8, DR80 adsorption onto TEPA-PS, TETA-PS, or DETA-PS should be regarded as chemical adsorption but controlled by physical

adsorption because their Q_{st} values were not much greater than 80kJ/mol.[43] In addition, we discovered that the Q_{st} values of the three systems increased with increasing the relevant Q_e values, suggesting that the three biosorbents all have heterogeneous surfaces. At lower values of Q_e, low heats of adsorption are obtained due to strong adsorbate-adsorbate interactions. However, when the Q_e values enlarge, high heats of adsorption are observed because the adsorptions occur on the most active sites of adsorbents.

Conclusion

Three novel biosorbents (TEPA-PS, TETA-PS and DETA-PS) were effective on the removal of DR80. Moreover, their optimum preparation conditions were discovered, i.e. optimum reaction temperature and the amount of alkali are given as follows: T_1 = 60°C, V_1 = 20.0mL (1.25mol/L NaOH), T_2 = 65°C, V_2 = 20.0mL (0.125mol/L NaOH) for the TEPA-PS preparation; and T_1 = 60°C, V_1 = 20.0mL (1.25mol/L NaOH), T_2 = 65°C, V_2 = 30.0mL (0.125mol/L NaOH) for the TETA-PS and DETA-PS preparations. The process variables of the dye adsorption onto the modified PS have been optimized by central composite design, and the effects of process variables and their interaction in adsorption capacities were analyzed. The results implied that all the three process variables have a direct relationship for DR80 removal by the modified PS, and temperature (x_2) has the maximal contribution (71.92%, 82.03% and 86.84% for the TEPA-PS, TETA-PS and DETA-PS, respectively) for removing it. The numerical optimization function based on the *D*-optimality index was utilized to search the process variable values that could obtain the maximum response (679.96, 674.51 and 579.08 mg/g), which were in good agreement with their corresponding experimental values determined (690.18, 657.55 and 588.56 mg/g) for DR80 removal onto TEPA-PS, TETA-PS and DETA-PS, respectively.

The dye adsorption was analyzed with the aspects of thermodynamics and kinetic. The thermodynamics results indicated the spontaneous and endothermic nature of DR80 adsorption. Kinetic studies confirmed that pseudo second order model could be fitted well for the three systems. According to the analysis results of intraparticle diffusion and liquid film models, the intraparticle diffusion dominated the adsorption rates of the three adsorption processes at different conditions. In addition, the adsorption isotherm data were also analyzed by two-parameter models (Langmuir, Freundlich, Temkin and Dubinin-Radushkevich) and three-parameter models (Radke-Prausnitz and Sips). The results indicated that Langmuir model was the best fit, showing the maximum monolayer adsorption capacities of 719.42, 694.44 and 617.28 $mg \cdot g^{-1}$ at 348.15 K for DR80 removal by TEPA-PS, TETA-PS and DETA-PS, respectively. The study clearly shows that the modified PS is a feasible, effective, economic and promising candidate for the treatment of azo dyes wastewater.

Acknowledgements

Financial support from Open Fund (PLN1408) of State Key Laboratory of Oil and Gas Reservoir Geology and Exploitation (Southwest Petroleum University), Sichuan Provincial Science & Technology Fund for Distinguished Young Scholars (2012JQ0058), with the NSFC (20873104) and SKLOGRGE (PLN-ZL002, SWPU) is gratefully acknowledged.

References

1 J. S. Cao, J. X. Lin, F. Fang, M. T Zhang and Z. R. Hu, *Bioresource Technol.*, 2014, **163**, 199-205.

2 Y. H. Wu, M. L. Zhang, H. Y. Zhao, S. X. Yang and A. Arkin, *RSC Adv.*, 2014, **4**, 61256-61267.

3 S. W. Zhang, X. X. Wang, J. X. Li, T. Wen, J. Z. Xu and X. K. Wang, *RSC Adv.*, 2014, **4**, 63110-63117.

4 X. P. Wang, Z. M. Liu, X. P. Ye, K. Hu, H. Q. Zhong, J. F. Yu, M. Jin and Z. Y. Guo, *Appl. Surf. Sci.*, 2014, **308**, 82-90.

5 X. Y. Yang, Z. Zhai, L. Xu, M. Z. Li, Y. Zhang and W. H. Hou, *RSC Adv.*, 2013, **3**, 3907-3916.

6 V. K. Gupta and Suhas, *J. Environ. Manage.*, 2009, **90**, 2313-2342.

7 H. J. Gao, Y. Wang and L. Q. Zheng, *Chem. Eng. J.*, 2013, **234**, 372-379.

8 T. Robinson, B. Chandran and P. Nigam, *Bioresource Technol.*, 2002, **85**, 119-124.

9 V. K. Gupta, R. Jain and S. Varshney, *J. Hazard. Mater.*, 2007, **142**, 443-448.

10 A. Abdolali, W. S. Guo, H. H. Ngo, S. S. Chen, N. C. Nguyen and K. L. Tung, *Bioresource Technol.*, 2014, **160**, 57-66.

11 D. Podstawczyk, A. W. Krowiak, K. Chojnacka and Z. Sadowski, *Bioresource Technol.*, 2014, **160**, 161-165.

12 A. B. Albadarin, J. Mo, Y. Glocheux, S. Allen, G. Walker and C. Mangwandi, *Chem. Eng. J.*, 2014, **255**, 525-534.

13 Y. Liu, X. M. Sun and B. H. Li, *Carbohyd. Polym.*, 2010, **81**, 335-339.

14 M. Şaban Tanyildizi, *Chem. Eng. J.*, 2011, **168**, 1234-1240.

15 P. Brown, I. A. Jefcoat, D. Parrish, S. Gill and Elizabeth Graham, *Adv. Environ. Res.*, 2000, **4**, 19-29.

16 E. I. El-Shafey, *J. Environ. Manage.*, 2007, **84**, 620-627.

17 C. S. Zhu, L. P. Wang and W. B. Chen, *J. Hazard. Mater.*, 2009, **168**, 739-746.

18 A. W. Krowiak, R. G. Szafran and S. Modelski, *Desalination*, 2011, **265**, 126-134.

19 S. W. Liao, C. I. Lin and L. H. Wang, *J. Taiwan Inst. Chem. E.*, 2011, **42**, 166-172.

20 H. R. Wu, C. I. Lin and L. H. Wang, *J. Taiwan Inst. Chem. E.*, 2011, **42**, 658-661.

21 R. M. Gong, M. Li, C. Yang, Y. Z. Sun and J. Chen, *J. Hazard. Mater.*, 2005, **121**, 247-250.

22 D. Özer, G. Dursun and A. Özer, *J. Hazard Mater.*, 2007, **144**, 171-179.

23 R. M. Gong, Y. Ding, M. Lie, C. Yang, H. J. Liu and Y.Z. Sun, *Dyes Pigments*, 2005, 64: 187-192.

24 M. Yue, M. Zhang, B. Liu, X. Xu, X. M. Li, Q. Y. Yue and C. Y. Ma, *Chinese J. Chem. Eng.*, 2013, **21**, 1260-1268.

25 Z. H. Ding, X.Hu, A. R. Zimmerman and B. Gao, *Bioresource Technol.*, 2014, **167**, 569-573.

26 J. Su, H. G. Huang, X.Y. Jin, X. Q. Lu and Z. L. Chen, *J. Hazard. Mater.*, 2011, **185**, 63-70.

27 A. Roy, B. Adhikari and S. B. Majumder, *Ind. Eng. Chem. Res.*, 2013, **52**, 6502-6512.

28 A. S. Bhatt, P. L. Sakaria, M. Vasudevan, R. R. Pawar, N. Sudheesh, H. C. Bajaj and H. M. Mody, *RSC Adv.*, 2012, **2**, 8663-8671.

29 J. Febrianto, A. N. Kosasih, J. Sunarso, Y. H. Ju, N. Indraswati and S. Ismadji, *J. Hazard. Mater.*, 2009, **162**, 616-645.

30 S. H. Chen, Q. Y.Yue, B. Y. Gao and X. Xu, *J. Colloid Interface Sci.*, 2010, **349**, 256-264.

31 M. Sarkar and P. Majumdar, *Chem. Eng. J.*, 2011, **175**, 376-387.

32 M. Roosta , M. Ghaedi, A. Daneshfar, R. Sahraei and A. Asghari, *Ultrason. Sonochem.*, 2014, **21**, 242-252.

33 A. A. Oladipo, M. Gazi and S. S. Samandari, *J. Taiwan Inst. Chem. E.*, 2014, **45**, 653-664.

34 Z. J. Cheng, L. Zhang, X. Guo, X. H. Jiang and T. Li, *Spectrochim. Acta Part A*, 2015, **137**: 1126-1143.

35 M. T. Yagub, T. K. Sen, S. Afroze and H. M. Ang, *Adv. Colloid Interface*, 2014, **209**, 172-184.

36 L. Eskandarian, M. Arami and E. Pajootan, *J. Chem. Eng. Data*, 2014, **59**, 444-454.

37 B. Kiran and A. Kaushik, *Biochem. Eng. J.*, 2008, **38**, 47-54.

38 S. Ghorai, A. Sarkar, M. Raoufi, A. B. Panda, H. Schönherr and S. Pal, *ACS Appl. Mater. Inter.*, 2014, **6**, 4766-4777.

39 J. R. Deka, C. L. Liu, T. H. Wang, W. C. Chang and H. M. Kao, *J. Hazard. Mater.*, 2014, **278**, 539-550.

40 R. Kumar, J. Rashid and M. A. Barakat, *RSC Adv.*, 2014, **4**, 38334-38340.

41 B. Singha and S. K. Das, *Colloid. Surface B*, 2013, **107**, 97-106.

42 G. G. Chang, Z. B. Bao, Z. G. Zhang, H. B. Xing, B. G. Su, Y. W.Yang and Q. L. Ren, *Ind. Eng. Chem. Res.*, 2014, **53**, 8592-8598.

43 G. K. Parshetti, S. Chowdhury and R. Balasubramanian, *Bioresource Technol.*, 2014, **161**, 310-319.

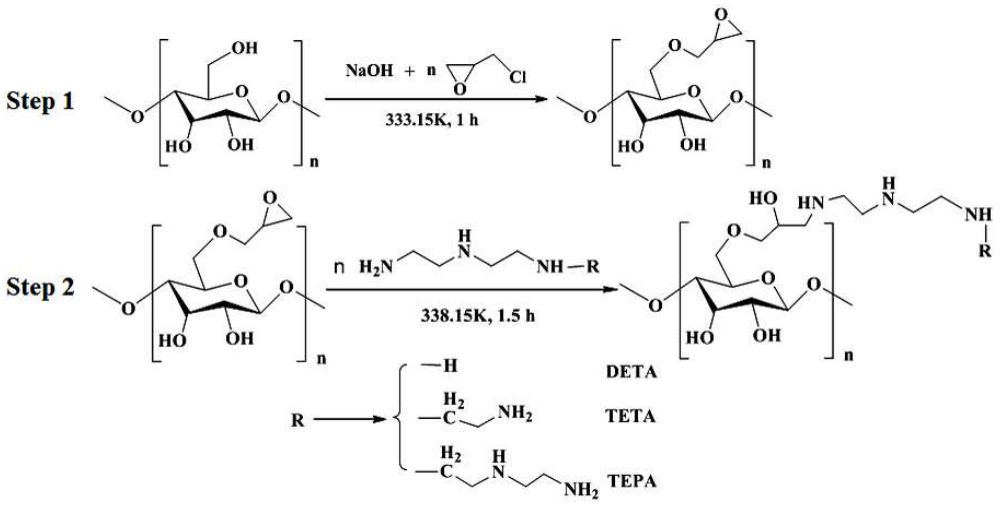

Fig. 1 The associated reactions of modification process of PS.

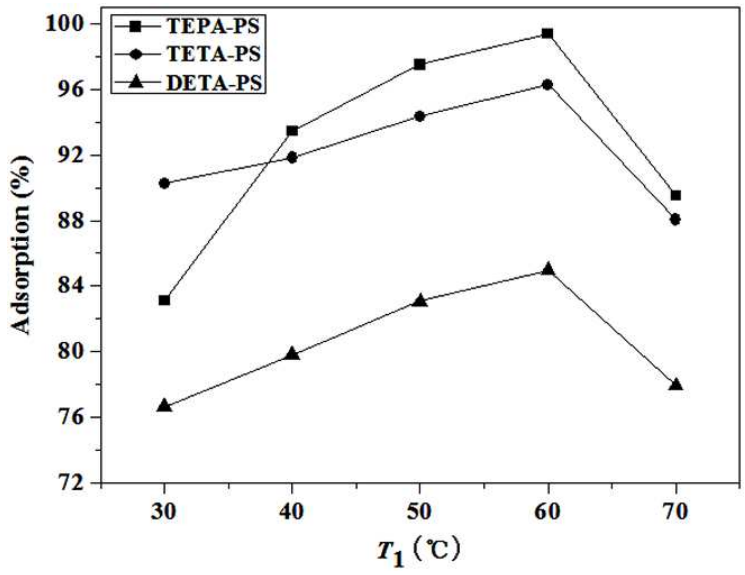

Fig. 2 Preparation of various biosorbents with different temperatures in the first step of the reactions for DR80 adsorption (in the first step: V_1 = 20.0mL of 1.25mol/L NaOH, t_1 = 60min; in the second step: V_2 = 20.0mL of 0.125mol/L NaOH, T_2 = 65°C, t_2 = 90min; adsorption conditions: adsorbent dosage = 20.0mg/100mL, [DR80] = 110mg/L, pH = 2.0, T = 50°C, t = 180min).

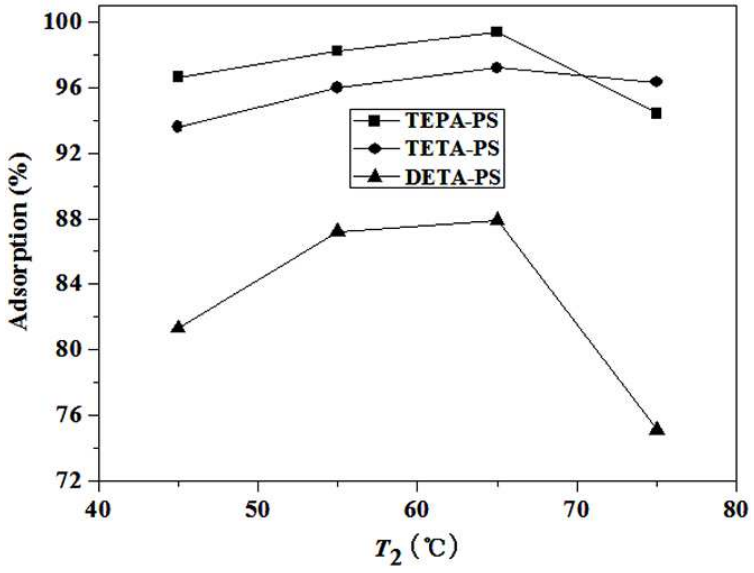

Fig. 3 Preparation of various biosorbents with different temperatures in the second step of the reactions for DR80 adsorption (in the first step: V_1 = 20.0mL of 1.25mol/L NaOH, T_1 = 60°C, t_1 = 60min; in the second step: V_2 = 20.0mL of 0.125mol/L NaOH, t_2 = 90min; adsorption conditions: adsorbent dosage = 20.0mg/100mL, [DR80] = 110mg/L, pH = 2.0, T = 50°C, t = 180min).

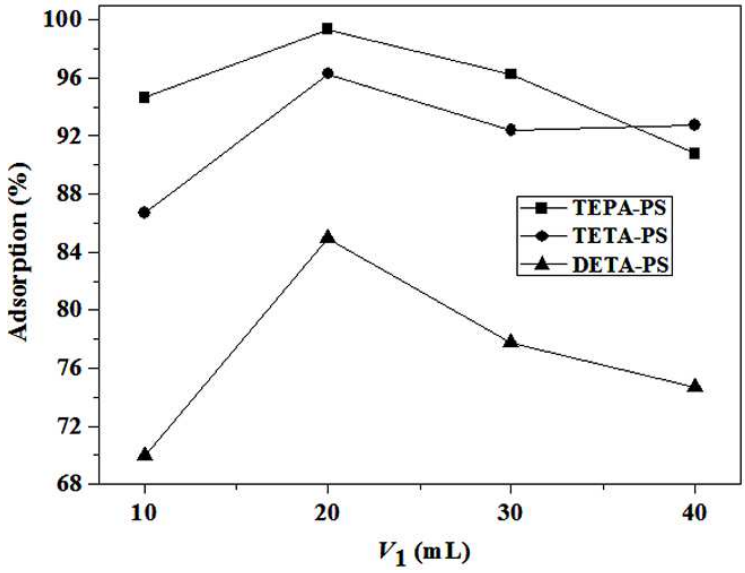

Fig. 4 Preparation of various biosorbents with different NaOH dosage in the first step of the reactions for DR80 adsorption (in the first step: [NaOH] = 1.25 mol/L, T_1 = 60°C, t_1 = 60min; in the second step: V_2 = 20.0mL of 0.125mol/L NaOH, T_2 = 65°C, t_2 = 90min; adsorption condition: adsorbent dosage = 20.0mg/100mL, [DR80] = 110mg/L, pH = 2.0, T = 50°C, t = 180min).

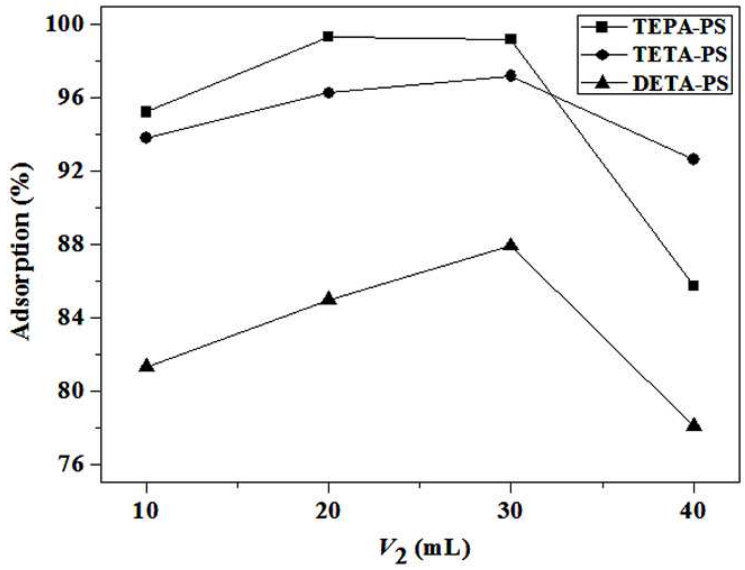

Fig. 5 Preparation of various biosorbents with different NaOH dosage in the second step of the reactions for DR80 adsorption (in the first step: V_1 = 20.0mL of 1.25mol/L NaOH, T_1 = 60°C, t_1 = 60min; in the second step: [NaOH] = 0.125 mol/L, T_2 = 65°C, t_2 = 90min; adsorption condition: adsorbent dosage = 20.0mg/100mL, [DR80] = 110mg/L, pH = 2.0, T = 50°C, t = 180min).

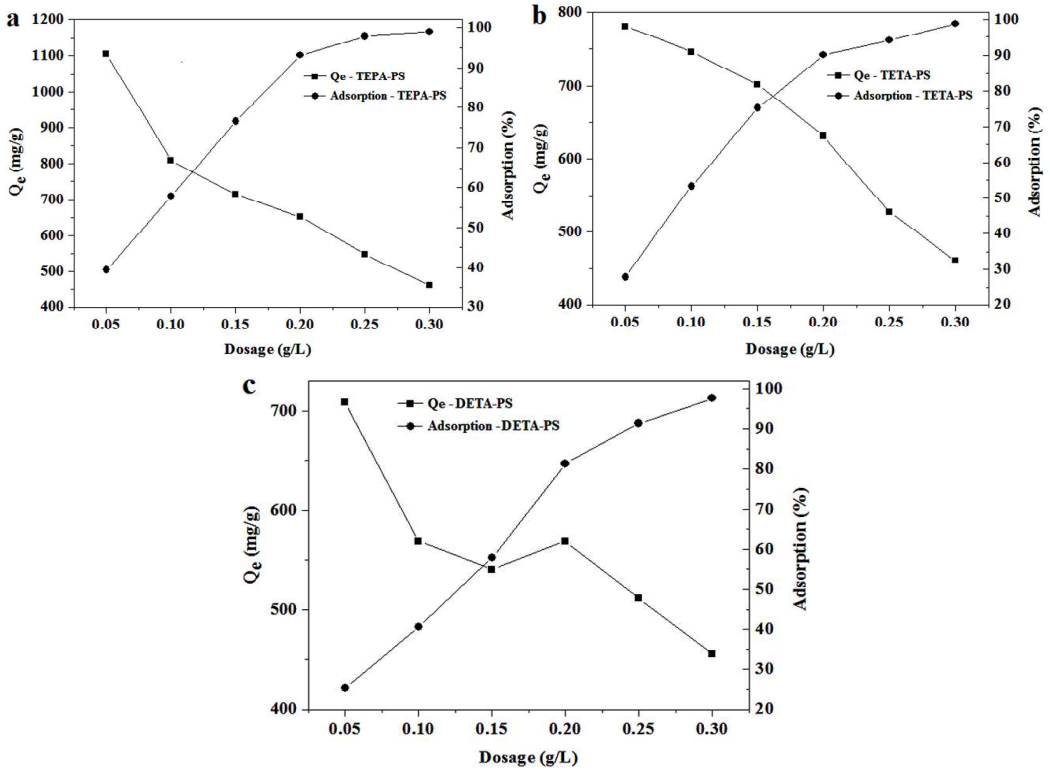

Fig. 6 The effect of adsorbent dosage for DR80 adsorption onto TEPA-PS (a), TETA-PS (b), and DETA-PS (c) (initial concentration of DR80 = 140 mg/L, pH = 2.0, T = 70°C and t = 180min).

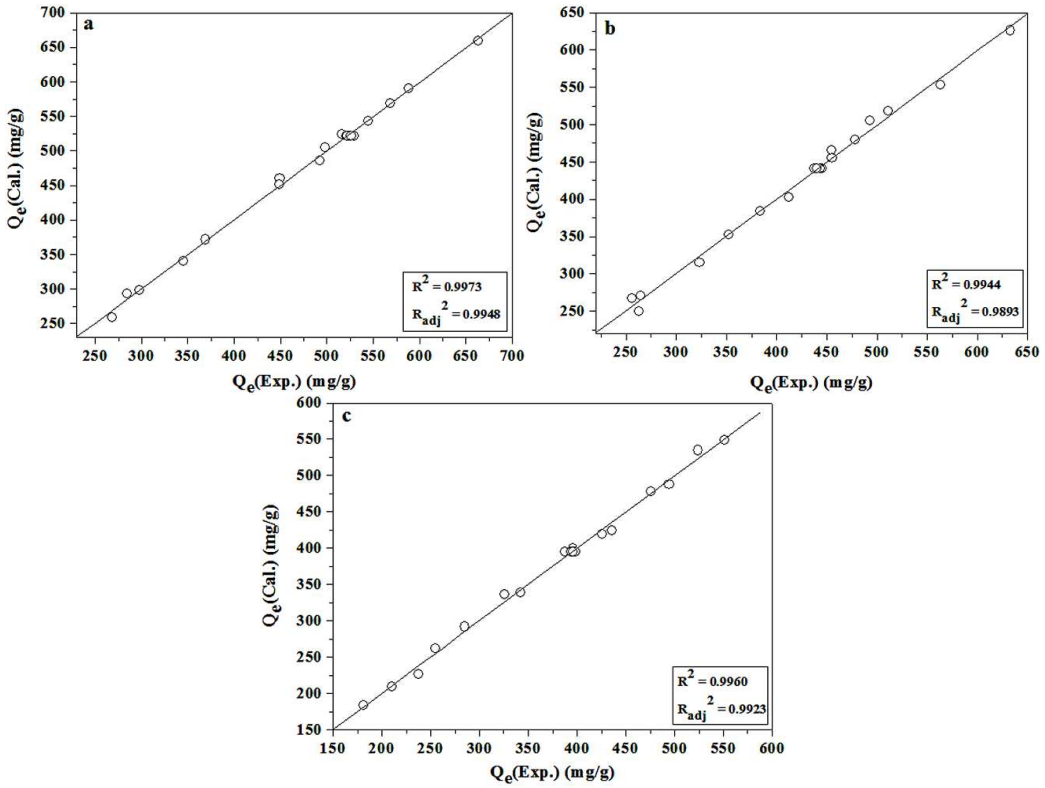

Fig. 7. Predicted *vs*. experimental values of the training set for DR80 adsorption onto TEPA-PS (a), TETA-PS (b), or DETA-PS (c).

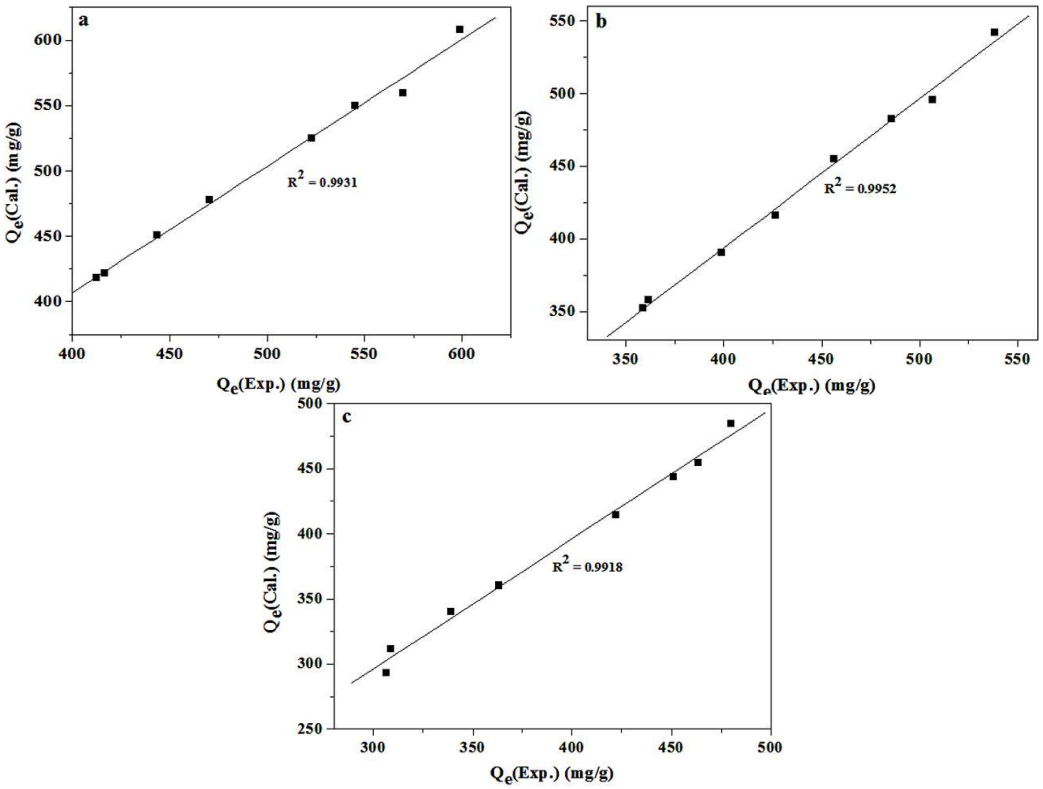

Fig. 8. Predicted *vs*. experimental values of the validation set for DR80 adsorption onto TEPA-PS (a), TETA-PS (b), or DETA-PS (c).

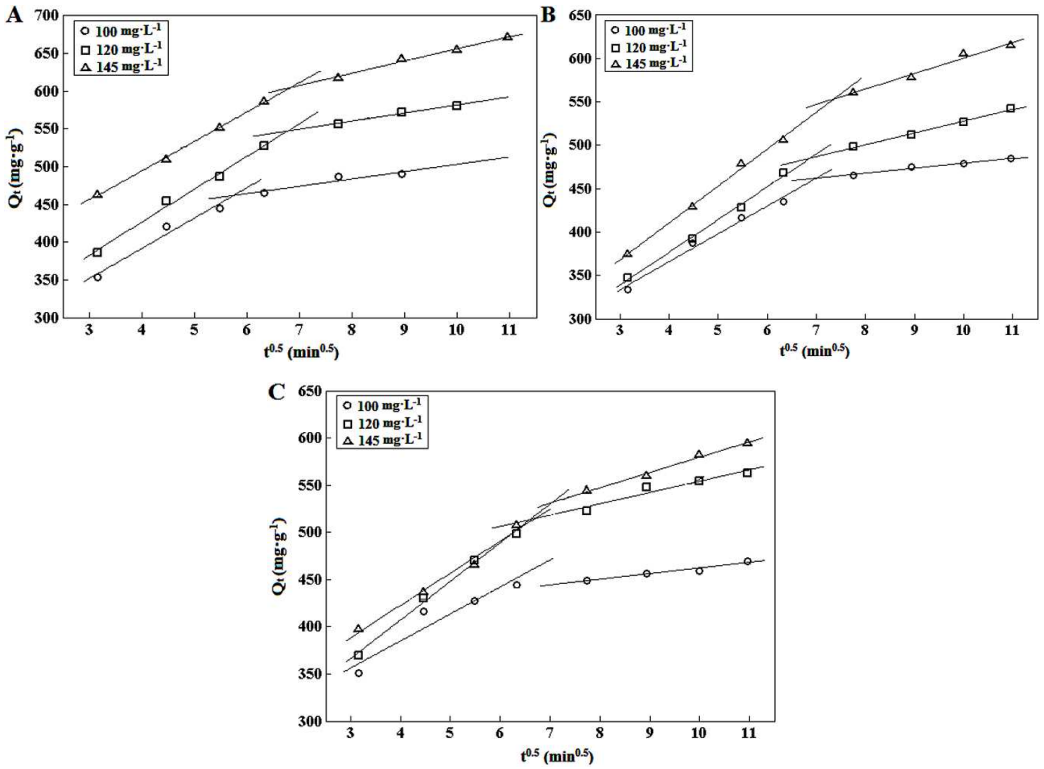

Fig. 9. Intraparticle diffusion model for DR80 by TEPA-PS (A), TETA-PS (B), or DETA-PS (C) at different initial concentrations of the dye (adsorbent dose = 20.0 mg/100mL, pH = 2.0, *T* = 75°C, agitation speed = 180 rpm for the DR80 system).

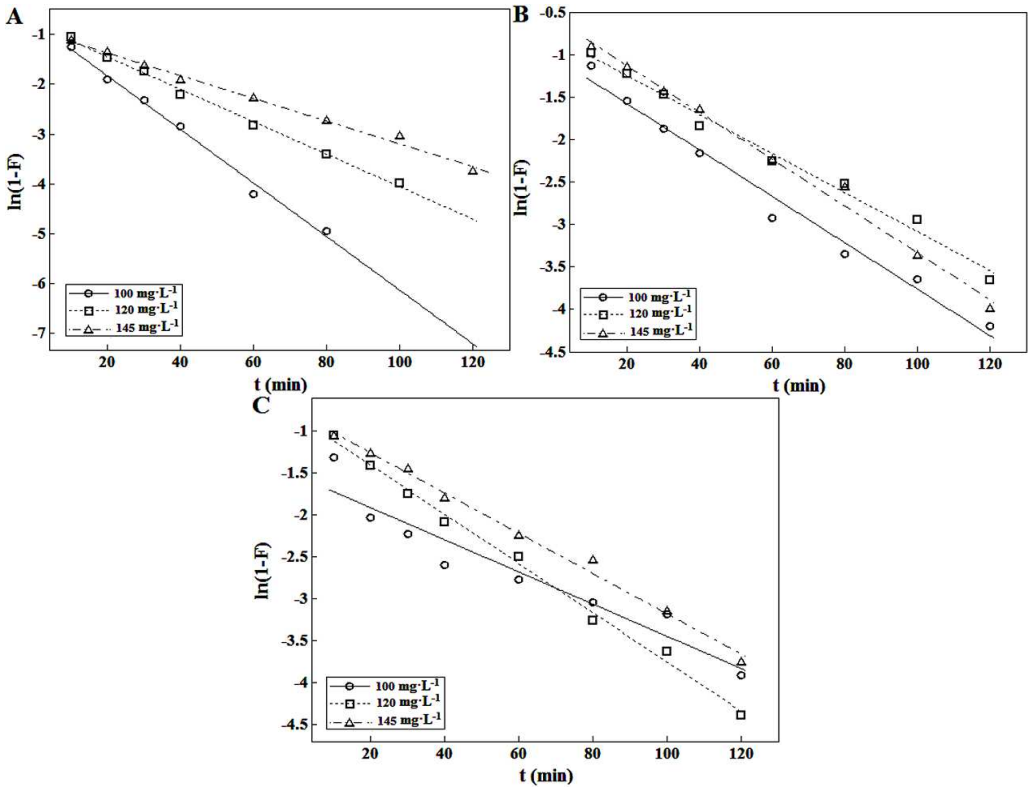

Fig. 10. Liquid film diffusion model for DR80 by TEPA-PS (A), TETA-PS (B), or DETA-PS (C) at different initial concentrations of the dye (adsorbent dose = 20.0 mg/100mL, pH = 2.0, T = 75°C, agitation speed = 180 rpm for the DR80 system).

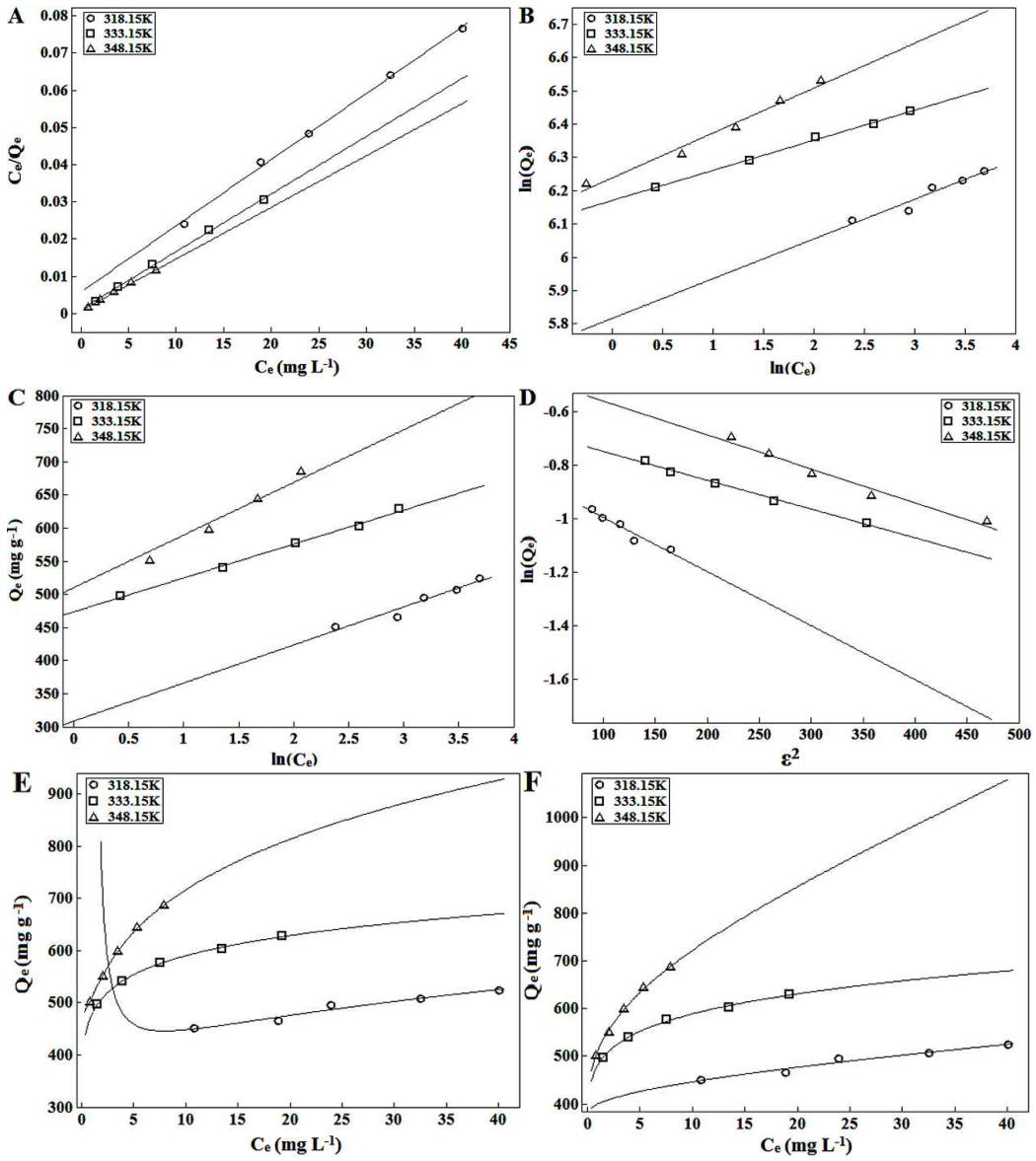

Fig. 11. Adsorption isotherms of DR80 onto TEPA-PS using Langmuir (A), Freundlich (B), Temkin (C), Dubinin-Radushkevich (D), Redlich-Peterson (E), or Sips (F) models at different temperatures (adsorbent dose = 20.0 mg/100mL, pH = 2.0, T = 75°C, t = 161min, agitation speed = 180 rpm).

Table 1 Experimental range and levels of operating parameters for the TEPA-PS, TETA-PS and DETA-PS systems.

Operating parameters	Coded variables	Variable levels				
		-1.25	-1	0	+1	+1.25
Initial concentration of the dye (mg/L)	x_1	95	100	120	140	145
Temperature (°C)	x_2	25	30	50	70	75
Time (min)	x_3	49	60	105	150	161

Table 2 Comparison of adsorption parameters for the DR80 by different biosorbents (C_{DR80} = 140mg/L, pH = 2.0, T = 70°C, t =150min).

	biosorbent			
	PS	TEPA-PS	TETA-PS	DETA-PS
Q_e (mg/g)	159.88	651.86	630.68	569.06
Adsorption (%)	22.84	93.12	90.10	81.29

Table 3 CCD matrix with three independent variables (coded values) and their corresponding experimental data for the TEPA-PS, TETA-PS and DETA-PS systems.

Run	Factor			Adsorption capacity (mg·g-1)											
				TEPA-PS				TETA-PS				DETA-PS			
	x_1	x_2	x_3	Exp.1	Exp.2	Exp.3	Average	Exp.1	Exp.2	Exp.3	Average	Exp.1	Exp.2	Exp.3	Average
1	0	0	0	522.98	522.66	521.66	522.43	450.45	443.07	442.82	445.45	395.57	393.65	396.85	395.36
2	+1.25	0	0	515.12	517.36	515.38	515.95	453.82	459.60	450.96	454.79	393.81	396.37	397.12	395.77
3	0	0	-1.25	447.24	454.62	445.52	449.13	386.59	381.45	383.64	383.89	327.54	324.97	325.75	326.09
4	-1.25	0	0	449.33	451.25	445.20	448.59	409.85	414.02	412.72	412.20	342.14	344.06	340.52	342.24
5	+1	+1	+1	664.38	665.02	660.59	663.33	633.57	633.89	631.45	632.97	547.24	555.26	550.68	551.06
6	-1	-1	-1	294.93	301.99	297.35	298.09	263.48	267.33	262.62	264.48	181.00	182.28	180.38	181.22
7	-1	+1	+1	499.04	499.36	495.86	498.09	493.90	493.26	490.98	492.71	477.21	475.29	474.38	475.63
8	+1	-1	-1	272.53	267.07	266.54	268.71	262.90	263.54	261.80	262.75	209.31	210.59	211.83	210.58
9	0	-1.25	0	281.64	284.21	287.66	284.50	251.80	260.46	255.66	255.97	234.79	239.92	238.02	237.58
10	-1	+1	-1	492.94	492.62	490.87	492.14	456.03	456.68	453.57	455.43	427.79	426.19	424.16	426.05
11	+1	+1	-1	567.46	567.78	568.68	567.97	510.01	510.65	512.81	511.16	490.12	498.14	495.55	494.60
12	0	0	0	529.40	527.79	530.05	529.08	436.65	436.97	438.02	437.21	384.98	390.76	386.28	387.34
13	0	0	0	526.51	524.58	522.96	524.68	443.71	440.18	445.55	443.15	390.76	400.39	396.73	395.96
14	0	0	0	520.41	521.69	522.43	521.51	444.35	444.67	440.98	443.33	390.76	397.82	392.74	393.77
15	-1	-1	+1	342.75	348.20	344.60	345.18	327.02	319.64	322.88	323.18	255.46	256.42	252.19	254.69
16	0	+1.25	0	586.84	588.77	589.56	588.39	566.94	563.41	560.72	563.69	520.41	528.43	522.88	523.91
17	0	0	0	522.02	522.98	520.88	521.96	436.01	441.46	435.65	437.71	400.39	396.53	398.48	398.47
18	0	0	+1.25	546.41	541.91	545.32	544.55	482.54	475.48	476.67	478.23	431.84	436.65	438.39	435.63
19	+1	-1	+1	369.45	370.09	367.44	368.99	354.04	352.12	350.55	352.24	286.97	284.72	282.91	284.87
20	0	0	0	522.98	528.75	526.75	526.16	437.93	446.92	435.11	439.99	397.50	395.25	393.66	395.47

Table 4 Taguchi design matrix with three independent variables in the validation set and their corresponding experimental data for the TEPA-PS, TETA-PS and DETA-PS systems.

Run	Variables			Adsorption capacity ($mg \cdot g^{-1}$)											
				TEPA-PS				TETA-PS				DETA-PS			
	C (mg/L)	*T* (℃)	*t* (min)	Exp.1	Exp.2	Exp.3	Average	Exp.1	Exp.2	Exp.3	Average	Exp.1	Exp.2	Exp.3	Average
1	110	40	80	406.87	415.85	414.95	412.56	358.73	357.77	359.54	358.68	306.42	305.78	307.47	306.56
2	110	40	140	445.38	444.09	441.15	443.54	400.45	397.56	398.21	398.74	335.30	344.93	336.58	338.94
3	110	60	80	524.33	522.72	520.64	522.56	458.86	454.69	455.32	456.29	424.84	420.03	421.69	422.19
4	110	60	140	546.79	541.34	546.78	544.97	505.71	506.03	508.01	506.58	469.77	459.50	461.30	463.52
5	130	40	80	413.63	420.07	415.26	416.32	361.17	362.45	360.73	361.45	300.83	316.88	308.34	308.68
6	130	40	140	469.96	474.45	467.32	470.58	426.96	424.71	427.48	426.38	365.34	363.74	360.96	363.35
7	130	60	80	569.13	569.77	570.81	569.90	483.44	489.54	484.22	485.73	454.24	446.85	451.77	450.95
8	130	60	140	596.41	600.90	599.38	598.90	535.43	541.21	537.67	538.10	476.06	485.04	479.63	480.24

Table 5 Kinetic parameters of four models at different concentration and temperature levels.

		TEPA-PS			TETA-PS			DETA-PS			TEPA-PS			TETA-PS			DETA-PS		
		T = 348.15K									C_0 = 145mg·L^{-1}								
model	parameter	C_0/mg·L^{-1}			C_0/mg·L^{-1}			C_0/mg·L^{-1}			T/K			T/K			T/K		
		100	120	145	100	120	145	100	120	145	318.15	333.15	348.15	318.15	333.15	348.15	318.15	333.15	348.15
pseudo first order	$Q_{e,fit}$/mg·g^{-1}	229.43	264.97	273.64	174.48	251.84	349.67	103.82	250.96	278.69	315.39	284.18	273.64	345.78	336.37	349.67	269.91	284.83	278.69
	k_1/min^{-1}	0.0537	0.0326	0.0228	0.0273	0.0229	0.0275	0.0192	0.0294	0.0240	0.0203	0.0201	0.0228	0.0201	0.0216	0.0275	0.0199	0.0213	0.0240
	R^2	0.9924	0.9960	0.9924	0.9831	0.9880	0.9921	0.9161	0.9950	0.9930	0.9930	0.9890	0.9924	0.9683	0.9770	0.9921	0.9816	0.9735	0.9930
pseudo second order	$Q_{e,fit}$/mg·g^{-1}	520.83	625.00	714.29	510.20	574.71	666.67	480.77	595.24	632.91	555.56	625.00	714.29	471.70	588.24	666.67	462.96	588.24	632.91
	$Q_{e,exp}$/mg·g^{-1}	493.58	591.66	687.13	491.98	556.35	626.80	479.46	569.83	608.18	528.59	611.39	687.13	426.86	548.81	626.80	443.23	566.14	608.18
	$k_2(\times10^4)$ /g·(mg·min)$^{-1}$	3.92	2.23	1.85	3.22	1.95	1.40	5.78	2.26	1.78	1.22	1.60	1.85	0.81	1.14	1.40	1.44	1.55	1.78
	R^2	0.9999	0.9996	0.9991	0.9998	0.9990	0.9985	0.9998	0.9997	0.9985	0.9968	0.9985	0.9991	0.9904	0.9934	0.9985	0.9942	0.9991	0.9985
	h/ mg·(g·min)$^{-1}$	106.34	87.11	94.39	83.82	64.41	62.22	133.60	80.07	71.30	37.65	62.50	94.39	18.02	39.45	62.22	30.86	53.63	71.30
second order	$Q_{e,fit}$/mg·g^{-1}	13.42	68.03	158.7	56.49	1428.6	73.53	357.14	44.25	116.28	400.0	526.3	158.7	285.7	238.1	73.5	270.3	243.9	116.3
	k_2/g·(mg·min)$^{-1}$	0.0039	0.0009	0.0005	0.0011	0.0005	0.0007	0.0007	0.0011	0.0005	0.0003	0.0003	0.0005	0.0003	0.0003	0.0007	0.0003	0.0004	0.0005
	R^2	0.8788	0.9030	0.8407	0.9153	0.8335	0.8105	0.8491	0.8224	0.8355	0.9049	0.9314	0.8407	0.7665	0.8646	0.8105	0.8042	0.8281	0.8355
Elovich	α/mg·(g·min)$^{-1}$	1632.6	802.4	1763.3	1666.6	578.6	382.1	29378.3	951.4	866.7	136.1	438.8	1763.3	42.1	160.4	382.1	132.6	234.3	866.7
	β/g·mg^{-1}	0.0151	0.0302	0.0116	0.0163	0.0124	0.0099	0.0238	0.0127	0.0120	0.0102	0.0107	0.0116	0.0101	0.0101	0.0099	0.0129	0.0102	0.0120
	R^2	0.9609	0.9595	0.9944	0.9752	0.9899	0.9945	0.8910	0.9866	0.9880	0.9964	0.9902	0.9944	0.9900	0.9830	0.9945	0.9851	0.9771	0.9880

Table 6 Isotherm parameters for DR80 adsorption onto TEPA-PS, TETA-PS, or DETA-PS.

		TEPA-PS			TETA-PS			DETA-PS		
			T/K			*T*/K			*T*/K	
model	parameter	318.15	333.15	348.15	318.15	333.15	348.15	318.15	333.15	348.15
Langmuir	Q_{max}/mg·g^{-1}	561.80	645.16	719.42	500.00	578.03	694.44	502.51	581.40	617.28
	K_L/ L·mg^{-1}	0.27	1.41	1.99	0.29	0.51	1.03	0.13	0.32	1.13
	R_L	0.0310-0.0218	0.0068-0.0047	0.0053-0.0037	0.0330-0.0232	0.0190-0.0133	0.0095-0.0067	0.0708-0.0504	0.0300-0.0211	0.0087-0.0061
	R	0.9990	0.9995	0.9984	0.9999	0.9994	0.9994	0.9999	0.9988	0.9999
Freundlich	K_F /mg·g^{-1}	336.64	477.99	511.27	308.99	383.33	450.61	226.17	338.70	443.63
	n	8.33	10.00	7.14	9.09	10.00	7.14	5.88	7.69	10.00
	R	0.9719	0.9989	0.9923	0.9916	0.9811	0.9960	0.9981	0.9857	0.9731
Temkin	K_T/ L·mg^{-1}	216.12	10460.14	611.63	415.87	1106.77	216.08	10.52	122.51	3412.64
	b_T/ kJ·mol^{-1}	0.0461	0.0542	0.0364	0.0562	0.0531	0.0355	0.0379	0.0433	0.0542
	R	0.9701	0.9980	0.9862	0.9933	0.9799	0.9970	0.9989	0.9827	0.9771
Dubinin-Radushkevich	Q_m/mmol·g^{-1}	0.4524	0.5272	0.6488	0.3997	0.4682	0.6240	0.4152	0.4774	0.5181
	β/mmol^2·J^{-2}	0.0020	0.0011	0.0013	0.0020	0.0015	0.0015	0.0034	0.0020	0.0012
	E/ kJ·mol^{-1}	15.81	21.32	19.61	15.81	18.26	18.26	12.13	15.81	20.41
	R	0.9642	0.9964	0.9840	0.9960	0.9786	0.9967	0.9992	0.9809	0.9844
Redlich-Peterson	K_{RP}/L·g^{-1}	-211.5	-2.22e+5	-3769.0	-8.32e+6	-3600.0	-2.963e+7	-7.636e+4	-312.1	-2.20e+5
	β_{RP}	0.7905	0.9080	0.8056	0.8944	0.8889	0.8581	0.8322	0.8009	0.9041
	α_{RP}/L·mg^{-1}	-0.9261	-465.3	-8.387	-2.685e+4	-9.716	-6.565e+4	-336.9	-1.236	-493.5
	R	0.9819	0.9987	0.9998	0.9913	0.9807	0.9965	0.9981	0.9887	0.9708
Sips	K_s/L·g^{-1}	122.2	423.0	-818.4	181.9	209.1	671.3	65.1	0.2055	720.9
	β_s	0.0337	0.0793	-0.1650	0.8965	0.0482	0.2553	1.0260	5.407e-5	1.0480
	α_s/L·mg^{-1}	-0.6489	-0.1160	-2.596	0.3600	-0.4642	0.5163	0.1286	-0.9994	1.1730
	R	0.9754	0.9987	0.9990	0.9991	0.9807	0.9969	0.9976	0.9872	0.9954

Table 7 Thermodynamic parameters and sticking probability for DR80 removal onto TEPA-PS, TETA-PS, or DETA-PS.

System	T (K)	ΔG^0 (kJ·mol^{-1})	ΔH^0 (kJ·mol^{-1})	ΔS^0 (J·mol^{-1}·K^{-1})	R^*	E_a (kJ·mol^{-1})	S^*	R^{**}
	318.15	-6.80						
TEPA-PS	333.15	-9.66	58.05	203.61	0.9990	49.79	1.92E-09	0.9966
	348.15	-12.92						
	318.15	-5.83						
TETA-PS	333.15	-7.70	50.11	175.09	0.9809	39.74	1.16E-07	0.9715
	348.15	-11.13						
	318.15	-5.48						
DETA-PS	333.15	-7.49	33.29	122.05	0.9975	24.19	4.11E-05	0.9996
	348.15	-9.13						

R^* is the correlation coefficient for the van't Hoff plot

R^{**} is the correlation coefficient for ln (1−θ) versus 1/T plot.

Table 8 Isosteric heats of DR80 adsorption onto TEPA-PS, TETA-PS, or DETA-PS.

biosorbent	Q_e/mg·g^{-1}	Q_{st}/kJ·mol^{-1}	R
	405.00	83.17	0.9615
	425.00	85.29	0.9616
TEPA-PS	445.00	88.36	0.9632
	465.00	91.60	0.9627
	495.00	99.19	0.9628
	405.00	73.00	0.9993
	425.00	78.14	0.9997
TETA-PS	445.00	85.34	0.9999
	465.00	96.67	0.9995
	495.00	152.78	0.9838
	405.00	90.19	0.9999
	425.00	94.21	0.9999
DETA-PS	445.00	100.06	0.9998
	465.00	109.57	0.9985
	495.00	152.74	0.9850